

Synthesis of light-harvesting dendrimers focally anchored with crown ethers or terpyridine ligands

Yongchun Pan,^a Meng Lu,^a Zhonghua Peng^{*a} and Joseph S. Melinger^b

^a Department of Chemistry, University of Missouri-Kansas City, 5100 Rockhill Road, Kansas City, MO 64110, USA. E-mail: pengz@umkc.edu

^b Naval Research Laboratory, Electronics Science and Technology Division, Code 6812, Washington, DC 20375, USA

Received 2nd July 2003, Accepted 10th October 2003

First published as an Advance Article on the web 31st October 2003

Crown ethers and terpyridine ligands have been successfully attached to the focal point of light harvesting phenylacetylene monodendrons through Pd-catalyzed coupling reactions. The structures of these functional monodendrons were characterized by ¹H and ¹³C NMR spectroscopy, mass spectrometry and elemental analysis. Such binding-ligand anchored dendrons exhibit broad absorption, large molar extinction coefficients and high fluorescence quantum yields. Coordination of crown ethers with alkali ions results in a significant increase in absorption strength in the UV range, but little alteration in either intensity or position of fluorescence emission. Coordination of terpyridine ligands with Ru²⁺, however, does efficiently quench the fluorescence from the dendrons, albeit only the smallest dendron exhibits efficient binding.

Introduction

Dendrimers have been extensively studied for well over a decade.¹ Not only have a great number of dendritic molecules been prepared through well-developed synthetic methodologies, interesting properties associated with the unique dendritic structures have been explored as well.² One particular application involves using dendrimers as synthetic light-harvesting antennae,^{3–5} which can serve as a model system for mimicking the energy transduction events in natural photosynthetic systems. A variety of light-harvesting dendrimers have been synthesized and their efficient energy transfer properties demonstrated.^{3–5} In light-harvesting dendrimers, the energy that is collected at the periphery over a broad range of irradiation is transferred convergently to an energy acceptor at the focal point and emitted as fluorescence in a narrow wavelength range. Both the intensity and the wavelength of the fluorescence emission at the locus may be designed to be responsive to environmental changes, making such dendrimers good candidates for fluorescence sensors.⁶

We have recently described a novel unsymmetrical phenylacetylene (PA) monodendron that exhibits broad absorption, large molar extinction coefficients, high fluorescence quantum yields, and high energy transfer efficiencies, making the unsymmetrical dendrimers efficient light-harvesting antennas.^{7,8} In addition, the presence of a phenolic hydroxy group at the focal point allows site-specific functionalization with a wide variety of structural units to realize functional dendrimers. Herein we report the detailed synthesis and optical properties of unsymmetrical dendrimers functionalized with crown ethers or terpyridine ligands at the locus. It is envisioned that binding of crown ethers or the terpyridine ligands with metal ions will alter the fluorescence from the dendron segments, thus making them fluorescence-based ion-sensors. In addition to their applications as sensors, these dendrimers are also interesting systems for self-assembly studies relating to nanoscale materials.⁹

Results and discussion

Chart 1 shows the structures of the two sets of dendrons, one focally anchored with benzo-crown ethers and the other with terpyridine units. The dendritic skeleton is based on *para*- and *meta*-branched phenylacetylenes.⁷

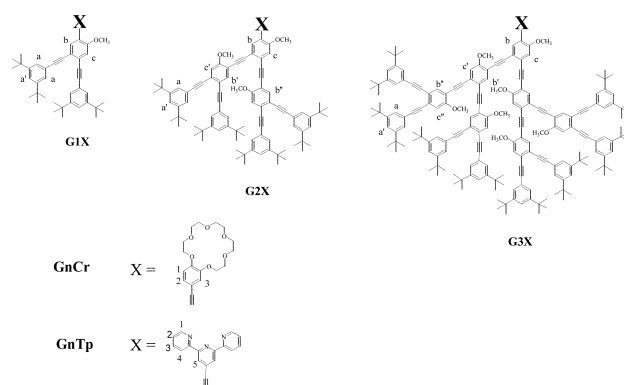
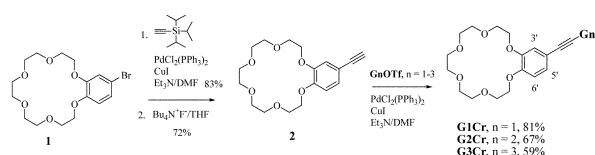


Chart 1 Structures of crown ether and terpyridine anchored monodendrons.

Synthesis of crown-ether terminated monodendrons (GnCr)

The synthesis of unsymmetrical conjugated monodendrons with a triflate functional group at the locus **GnOTf** (X = OTf in Chart 1, *n* = 1–3) has been reported previously.^{7,10} Crown ether functionalized monodendrons were synthesized by the Sonogashira coupling reaction of acetylene compound **2** with **GnOTf**.¹¹ As shown in Scheme 1, compound **2** was synthesized by the coupling reaction of bromobenzocrown ether **1** with tri(isopropyl)silyl acetylene at 80 °C, followed by desilylation with tetrabutylammonium fluoride. The overall yield is 60%. When trimethylsilylacetylene, a compound with a much lower boiling point, is used, however, the coupling reaction was slow and incomplete. The reaction of compound **2** with **GnOTf** went smoothly. While the yields decrease gradually from lower generation to higher generation dendrons, good yields were obtained even for the third generation dendron. Unreacted triflates were easily removed by chromatography due to their

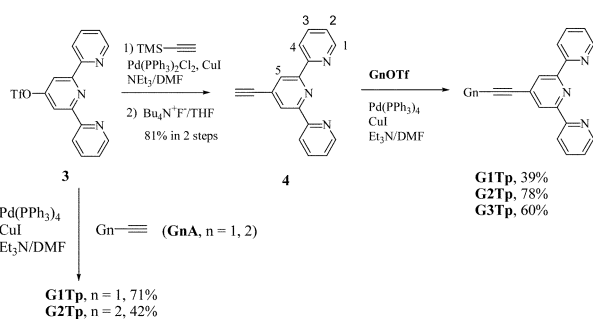


Scheme 1 Synthesis of crown ether functionalized monodendrons.

significantly lower polarity than the crown ether anchored products.

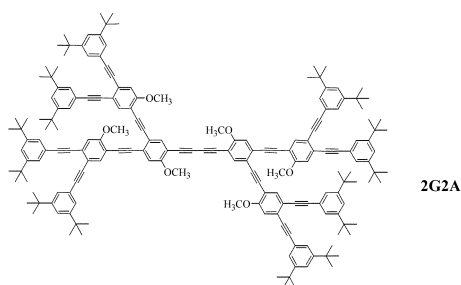
Synthesis of *G_nTp*

To attach a terpyridine ligand to the dendron core, an acetylene-functionalized terpyridine compound **4** was prepared according to Scheme 2. The Sonogashira coupling reaction of **4** with *G_nOTf* was not successful when Pd(PPh₃)₂Cl₂ was used as the catalyst. However, the reaction can be promoted by simply switching the palladium catalyst to Pd(PPh₃)₄.¹² It was found that, in the coupling reactions of triflates, it was beneficial to use DMF as the solvent and a minimum amount of triethylamine as the base.¹⁰ In DMF with about 10–20 equivalents of amine relative to reactants, the reaction of triflates *G_nOTf* and acetylene terminated terpyridine **4** behaved quite well and the target functional dendrons were obtained in moderate to good yields.



Scheme 2 Synthesis of terpyridine functionalized monodendrons.

An alternative route to terpyridine functionalization monodendrons uses the reaction of terpyridine triflate **3** and the acetylene terminated monodendrons *G_nA* (X is ethynyl in Chart 1). *G_nA* can be readily synthesized by converting the focal triflate functional group in *G_nOTf* to the ethynyl group.¹⁰ The presence of electron-withdrawing pyridine groups makes **3** more reactive than triflates of monodendrons, such as **G1OTf**. The reaction of **G1A** and **3** at 76 °C in triethylamine finished in two days and the product **G1Tp** was isolated in 71% yield after chromatography. Under the same conditions, however, the reaction of **G2A** and **3** took much longer. While the desired product **G2Tp** was obtained in 42% yield, a significant amount (17%) of self-coupling side product, **2G2A** was isolated. It appears that this alternative route works well only for the first generation dendron.



Structural characterizations of *G_nCr* and *G_nTp*

All *G_nCr* were soluble in common organic solvents such as chloroform, methylene chloride, THF, *etc.* They were characterized by ¹H NMR, ¹³C NMR, and MALDI-TOF mass spectrometry. In the ¹H NMR, characteristics of both benzo crown ether functionality and monodendrons can be easily identified. In the aromatic region, a well-isolated doublet at 6.84 ppm, corresponding to proton 1 (see Chart 1 for labeling), can be clearly seen even for **G3Cr**. The protons *ortho* to both acetylene groups (labeled as b, b', b'' in Chart 1) appear as singlets at low

fields ($\delta > 7.7$ ppm). MALDI-TOF mass spectrometry gives the correct masses for **G1Cr** and **G2Cr**. But for **G3Cr**, it gives a mass 23 units higher than the theoretical value, likely due to salt ions such as Na⁺ introduced either from the sample or the matrix.

Terpyridine-functionalized monodendrons show good solubility in common organic solvents as well. A stacked plot of aromatic regions of the ¹H NMR spectra of **G1Tp**, **G2Tp**, **G3Tp** and the ethynyl-substituted terpyridine compound **4**, is shown in Fig. 1. The signals can be grouped into four regions. Chemical shifts above 8.6 ppm are due to protons 1, 4, and 5 in the terpyridine segment (see Chart 1 and Scheme 2 for the labeling). These signals are well separated from those associated with protons in the PA dendrons. It is interesting to note that a significant downfield shift is observed for protons in the central pyridine ring (proton 5) when the PA dendrons are attached to the terpyridine segment, indicating a deshielding effect due to the electron delocalization from the central pyridine ring to the PA dendrons. The second region shows peaks with chemical shifts at 7.7–8.0 ppm. The triplet at 7.88 ppm is attributed to proton 2 in the two side pyridine rings. The aromatic protons *ortho* to both ethynyl groups (labeled as b, b', b'' in Chart 1) appear as singlets in this region. For **G1Tp** and **G2Tp**, these singlets are separated from the triplet. For higher-generation dendrons, however, they are severely overlapped. The third region shows chemical shifts at 7.30–7.40 ppm. Aromatic protons in the peripheral phenyl rings (labeled a, a' in Chart 1) give broad signals in this region. Proton 3 in the side pyridine rings also appears in this region. The fourth region includes signals with chemical shifts between 7.0–7.2 ppm, which are due to aromatic protons associated with the PA dendrons (protons labeled c, c', c'' in Chart 1). The structures of *G_nTp* are also confirmed by mass spectrometry and elemental analysis.

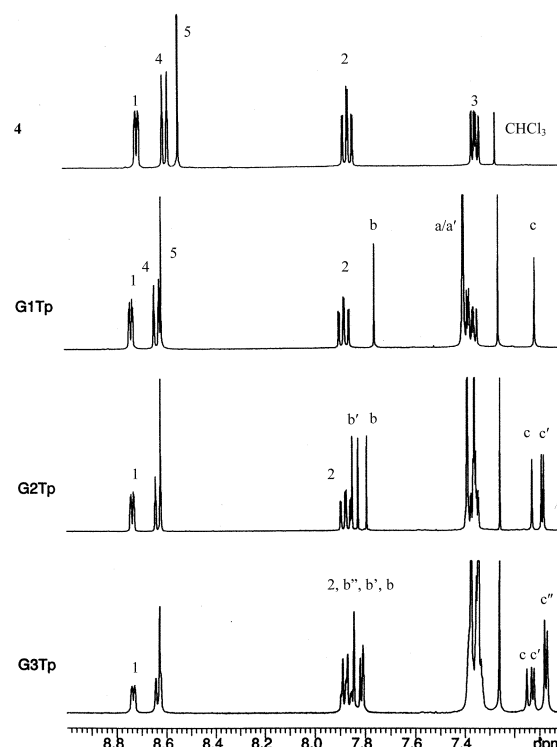


Fig. 1 Aromatic regions of ¹H NMR spectra of **4**, **G1Tp**, **G2Tp** and **G3Tp**.

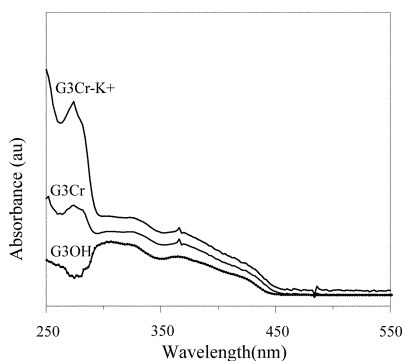
Optical properties of *G_nCr* and *G_nTp*

Fig. 2 shows the absorption spectra of **G3OH**, **G3Cr**, and **G3Cr** with excess KBr in methylene chloride solutions. The UV/Vis absorption spectra of *G_nCr* resemble those of *G_nOH* (X = OH in Chart 1). Compared to **G3OH**, **G3Cr** shows

Table 1 Optical properties of dendritic compounds

| Compound | $\lambda_{\text{edge}}^{\text{ab}}$ /nm | $\lambda_{\text{max}}^{\text{ab}}$ /nm | $\epsilon_{\text{max}}^{\text{c}}$ /M ⁻¹ cm ⁻¹ | $\lambda_{\text{max}}^{\text{em}}$ ^d /nm | $\phi_{\text{f}}^{\text{e}}$ | τ^{f} /ns |
|-------------|---|--|--|---|------------------------------|-----------------------|
| 4 | 338 | 242 | 47000 | 351 | — | — |
| G1Tp | 403 | 290 | 79000 | 423 | 0.77 | 2.1 |
| G2Tp | 438 | 322 | 111000 | 439 | 0.65 | 2.1 |
| G3Tp | 452 | 324 | 213000 | 451 | 0.49 | 1.7 |
| G1A | 376 | 276 | 48000 | 392 | 0.66 | 2.7 |
| G2A | 422 | 304 | 110000 | 425 | 0.84 | 2.4 |
| G1OH | 356 | 283 | 48000 | 360, 374 (sh) | 0.40 | 1.7 |
| G2OH | 416 | 299 | 82500 | 417, 438 (sh) | 0.81 | 2.0 |
| G3OH | 440 | 310 | 171000 | 440, 466 (sh) | 0.70 | 1.9 |
| G4OH | 453 | 321 | 330000 | 452, 479 (sh) | 0.65 | 1.7 |

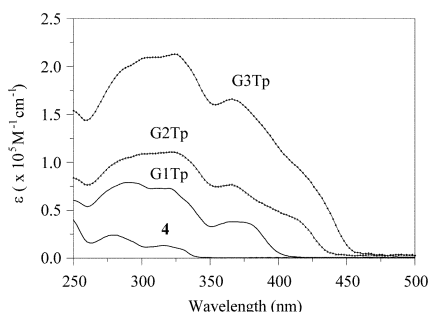
^a Absorption band edge. ^b Maximum absorption wavelengths. ^c Molar extinction coefficients at the absorption maximum. ^d Fluorescence emission wavelengths. ^e Fluorescence quantum yields. ^f Fluorescence lifetimes.

**Fig. 2** UV/Vis absorption spectra of **G3OH**, **G3Cr** and **G3Cr + K⁺**.

stronger absorptions in the shorter wavelength region. The absorptions in the longer wavelength range (350–440 nm) are nearly identical to those of **G3OH**. Even though the longest *para* conjugated segment in **G3Cr** is one phenyl acetylene unit longer than that of **G3OH**, the absorption edge is only slightly red shifted. Addition of **KBr** into the **G3Cr** solution results in a significant increase in the absorption strength at around 275 nm. However, little change is observed for the absorption at longer wavelengths. As a result, both the fluorescence intensity and wavelengths show no obvious change after **K⁺** coordination. This could result from either inefficient binding due to the steric crowding at the focal point or insufficient conformational change caused by binding of those ions due to the rigidity of the dendrons.

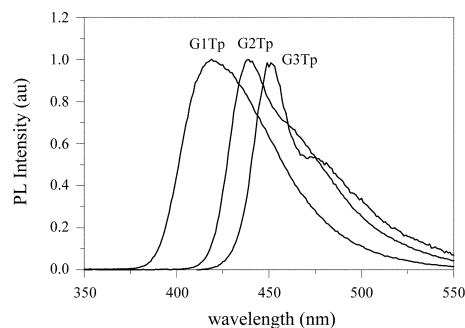
The optical properties of **G_nTp** in dilute methylene chloride solutions were studied by UV/Vis absorption, steady-state and time-resolved fluorescence measurements. The photophysical properties of these compounds are collected in Table 1. For comparison, the optical properties of **G_nA** and **G_nOH**, which have been reported previously,^{8,10} are also listed in the same table.

Fig. 3 shows the absorption spectra of **G_nTp** and the ethynyl substituted terpyridine **4** in methylene chloride. Clearly, the lowest excitation energy of **G_nTp** shifts to the red with increasing generations. The absorption edges for **G1Tp**, **G2Tp**, and

**Fig. 3** Absorption spectra of **4**, **G1Tp**, **G2Tp** and **G3Tp** in methylene chloride.

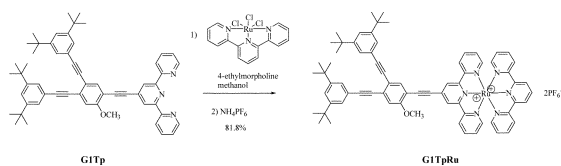
G3Tp are 403, 438, and 452 nm, respectively. Compared to **G1A** and **G2A**, the absorption band edges of **G1Tp** and **G2Tp** are red-shifted by 27 and 15 nm, respectively, indicating that the π conjugation extends from the main PA branch to the central pyridine ring, consistent with the ¹H NMR results. It is worth noting that the absorption band edges of **G_nTp** approach those of **G_n + 1OH**, except for the smallest dendron ($n = 1$). For example, **G3Tp** has an absorption band edge of 452 nm, nearly identical to that of **G4OH**.⁷

These terpyridine-anchored monodendrons exhibit relatively strong fluorescence. Their steady-state fluorescence emission spectra in methylene chloride solution are shown in Fig. 4. The emission spectra were obtained using an excitation wavelength of 350 nm. It should be pointed out that the emission maxima and shape of all these monodendrons do not change with variations of excitation wavelengths within their absorption profiles. As the size of the monodendron increases, the maximum emission wavelengths shift to the red, while the quantum yield decreases. As shown in Table 1, the fluorescence quantum yields for **G1Tp**, **G2Tp** and **G3Tp** are 77, 65, 49%, respectively. A similar trend is also observed for the **G_n + 1OH** monodendrons. The decreased quantum yields for higher-generation monodendrons are likely due to the stronger interactions between the different branches, which may also account for the slightly decreased fluorescence lifetimes with higher-generation dendrons.

**Fig. 4** Fluorescence emission spectra of **G_nTp**.

Coordination with Ru-complexes

Coordination of the PA dendron-attached terpyridine ligands with Ru-complexes was investigated. The ruthenium complex of **G1Tp** was prepared according to a reported procedure.¹³ As shown in Scheme 3, a mixture of **G1Tp**, terpyridine ruthenium trichloride and a drop of 4-ethylmorpholine was refluxed in methanol for 21 h to give a dark red solution, which was then treated with excess ammonium hexafluorophosphate to afford **G1TpRu** as a red solid after chromatography. Using the same procedure, however, we were not able to obtain the ruthenium complexes for **G2Tp** and **G3Tp**. Although the reason is not known, the steric hindrance at the focal point of these



Scheme 3 Synthesis of ruthenium complex **GITpRu**.

monodendrons may play a role. It is possible that the steric effect limits the bond angles of the terpyridine so that the desired bite angles for terpyridine with ruthenium could not be achieved. To overcome this problem, bipyridine ligands are being attached to the locus.

The structure of **GITpRu** was confirmed by NMR, MS, and elemental analysis. The FAB mass spectrum shows observed masses of m/z 1267 and 1123, corresponding to the loss of one and two PF_6^- ions, respectively. No molecular ion was observed. ^1H NMR spectra of **GITpRu** in CDCl_3 show well-resolved signals. The existence of two terpyridine groups is manifested by the appearance of many signals in pairs in the aromatic region. For example, there are two pairs of well-separated triplets, one at around 7.2 ppm and the other at 7.8 ppm, which can be assigned to protons 2/2' and 3/3', respectively. There is also one doublet, at around 7.3 ppm which is assigned to protons 4/4'. A lone triplet at 8.2 ppm is attributed to proton 6. The two protons (b and c) in the central phenyl ring give two singlets at 7.17 and 7.92 ppm. The protons in the two phenyl rings with *tert*-butyl substituents appear as two broad signals at 7.40 and 7.42 ppm.

After coordination of terpyridine with metal ion, the UV/Vis absorption spectrum reveals a new band at 498 nm, which is assigned to the MLCT band (Fig. 5).¹⁵ While **GITp** is highly fluorescent, the fluorescence of **GITpRu** at room temperature is barely detectable. The quenching efficiency is greater than 99%. These results suggest that terpyridine-anchored dendrons **GnTp** would be highly efficient fluorescence sensors had **GnTp** been able to bind with transition metal ions. To facilitate metal-ligand binding and to enhance emission from the MLCT state after coordination, efforts are being made to link bipyridine ligands, whose Ru- and Os-complexes are known to exhibit a strong and long-lived luminescence at room temperature in fluid solution,¹⁶ to the dendron locus.

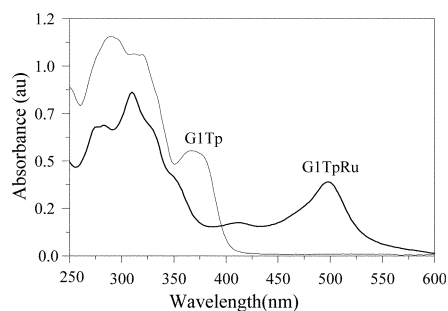


Fig. 5 Absorption spectra of **GITp** and **GITpRu**.

Conclusions

Taking advantage of the phenolic group at the PA dendron locus, crown ethers and terpyridine ligands have been successfully attached to the core of light-harvesting PA monodendrons. While coordination of crown ethers with alkali ions does not lead to significant alteration in either intensity or position of their fluorescence emission, coordination of terpyridine ligands with Ru^{2+} does efficiently quench the fluorescence from the dendrons, albeit only the smallest dendron exhibits efficient binding. The same synthetic approach can be applied to attach a variety of other units to the dendron locus to generate functional dendrimers.

Experimental

All reagents and solvents were obtained from either Aldrich or Fisher and were used as received unless otherwise stated. Anhydrous THF and acetonitrile were distilled prior to use from sodium metal/benzophenone. Triethylamine was distilled from calcium hydride prior to use. All air- and moisture-sensitive reactions were carried out under a N_2 atmosphere.

^1H NMR spectra were recorded on a Varian Unity 400 MHz spectrometer. UV/Vis absorption spectra were recorded using a Hewlett-Packard 8452A diode array spectrophotometer. The fluorescence emission spectra were measured using a Shimadzu RF-5301PC spectrofluorimeter. Fluorescence quantum yields were determined using quinine sulfate in 1 N H_2SO_4 ($\phi_f \approx 0.55$) as the standard.¹⁴ Time-dependent fluorescence measurements were performed using the technique of time-correlated single-photon counting (TCSPC).

Synthesis

The preparations of compounds **GnOH** ($n = 1-3$) and **GnOTf** ($n = 1-3$) were reported previously.⁷

4'-Ethylnylbenzo-18-crown-6 (2). An oven-dried flask was charged with 4'-bromobenzo-18-crown-6 (2.48 g, 6.332 mmol), triisopropylsilylacetylene (8.0 cm^3 , 35.66 mmol), $\text{Pd}(\text{PPh}_3)_2\text{Cl}_2$ (0.147 g, 0.209 mmol), copper(I) iodide (0.0243 g, 0.128 mmol), triethylamine (3.0 cm^3) and DMF (15.0 cm^3). The mixture was stirred at 80 °C overnight. The reaction mixture was then poured into 3 M hydrochloric acid (20 cm^3) and extracted with methylene chloride (3 \times 20 cm^3). The combined organic extracts were washed with water (3 \times 20 cm^3), brine (20 cm^3), dried over anhydrous sodium sulfate and evaporated *in vacuo*. The residue was then purified by chromatography, eluting with hexanes/ethyl acetate (3 : 1), followed by methylene chloride/methanol (20 : 1) to give triisopropylsilyl-protected precursor (2.59 g, 83%) as white crystals. δ_{H} (250 MHz; CDCl_3) 7.06 (1 H, d, J 8.6), 6.97 (1 H, s), 6.77 (1H d, J 8.6), 4.15–4.12 (4 H, m), 3.92–3.89 (4 H, m), 3.74–3.67 (12 H, m) and 1.12 (21 H, s). δ_{C} (62.5 MHz, CDCl_3) 149.6, 148.4, 125.9, 117.4, 116.2, 113.4, 107.2, 88.6, 70.9, 70.7, 69.5, 69.2, 69.0, 18.7 and 11.4. The precursor compound was desilylated by adding a sample of Bu_4NF (1.93 g, 6.10 mmol) to its THF solution (2.59 g, 5.27 mmol in 25 cm^3 of THF). The solution was stirred at room temperature for 30 min and poured into water. It was extracted with methylene chloride. The organic extracts were washed with water, dried over anhydrous sodium sulfate and evaporated *in vacuo* to give a yellow solid. It was then purified by passing through a short silica gel column, eluting with hexanes/ethyl acetate (3 : 1), followed by methylene chloride/methanol (25 : 1) to afford the title compound (1.28 g, 72%) as a white solid. δ_{H} (250 MHz, CDCl_3) 7.08 (1 H, dd, J 8.6 and 2.5), 6.99 (1 H, d, J 2.5), 6.79 (1 H, d, J 8.6), 4.17–4.12 (4 H, m), 3.94–3.89 (4 H, m), 3.78–3.68 (12 H, m) and 3.00 (1 H, s). δ_{C} (62.5 MHz, CDCl_3) 150.1, 148.6, 126.1, 117.5, 114.7, 113.5, 83.9, 75.9, 71.1, 70.9, 69.7, 69.2 and 69.1.

4'-Ethylnyl-2,2':6',2''-terpyridine (4). A solution of compound **3** (1.008 g, 2.64 mmol), trimethylsilylacetylene (0.80 cm^3 , 5.62 mmol), $\text{Pd}(\text{PPh}_3)_2\text{Cl}_2$ (0.123 g, 0.176 mmol), copper(I) iodide (0.0209 g, 0.110 mmol), triethylamine (2.0 cm^3) in DMF (5.0 cm^3) was stirred at 55 °C for 3 h and was then poured into water. The resulting aqueous solution was extracted with methylene chloride. The combined organic extracts were collected and dried over magnesium sulfate. After removal of the solvent, the crude product was purified by chromatography on aluminium oxide to give 4'-[(trimethylsilyl)ethynyl]-2,2':6',2''-terpyridine as a white solid. δ_{H} (400 MHz, CDCl_3) 8.73 (2 H, ddd, J 4.8, 1.6 and 1.2), 8.63 (2 H, dt, J 7.6 and 1.2), 8.58 (2 H, s), 7.88 (2 H, td, J 7.6 and 1.6), 7.36 (2 H, ddd, J 7.6, 4.8 and 1.2), 0.28 (9 H, s). δ_{C} (100 MHz, CDCl_3) 155.9, 155.7, 149.4, 137.1, 133.7, 132.2, 129.3, 128.7, 124.2, 123.1, 122.7, 121.5, 94.0

and 87.7. Compound **4** was prepared by the desilylation of 4'-[(trimethylsilyl)ethynyl]-2,2':6',2''-terpyridine using the same procedure as previously described. The overall yield for the two steps was 81%. δ_{H} (400 MHz, CDCl_3) 8.73 (2 H, ddd, J 4.8, 1.6 and 1.2), 8.63 (2 H, dt, J 7.6 and 1.2), 8.58 (2 H, s), 7.88 (2 H, td, J 7.6 and 1.6) and 7.36 (2 H, ddd, J 7.6, 4.8 and 1.2). δ_{C} (100 MHz, CDCl_3) 155.9, 155.7, 149.4, 137.1, 133.7, 132.2, 129.3, 128.7, 124.2, 123.1, 122.7, 121.5, 94.0 and 87.7.

G1Cr. A mixture containing **G1OTf** (0.149 g, 0.218 mmol), 4'-ethynylbenzo-18-crown-6 (0.0973 g, 0.289 mmol), $\text{Pd}(\text{PPh}_3)_2\text{-Cl}_2$ (0.0072 g, 0.0103 mmol), and copper(I) iodide (0.0046 g, 0.0242 mmol) in triethylamine (0.5 cm^3) and DMF (2.0 cm^3) was stirred at 60 °C for 6 h. After cooling to room temperature, the mixture was poured into water and extracted with CH_2Cl_2 . The organic layer was washed with an aqueous HCl solution and then dried over MgSO_4 . The crude product was purified by chromatography using silica gel eluting with 5 : 1 hexane/ethyl acetate to afford **G1Cr** (0.15 g, 81%) as a white solid. δ_{H} (250 MHz, CDCl_3) 7.70 (1 H, s), 7.39–7.37 (6 H, m), 7.14 (1 H, dd, J 8.6 and 2.5), 7.09 (1 H, s), 7.06 (1 H, d, J 2.5), 6.83 (1 H, d, J 8.6), 4.19–4.16 (4 H, m), 3.95–3.93 (7 H, m), 3.76–3.69 (12 H, m) and 1.28 (36 H, s). δ_{C} (62.5 MHz, CDCl_3) 159.1, 151.0, 150.9, 149.8, 148.6, 136.8, 132.3, 132.2, 128.8, 128.6, 127.0, 126.1, 126.0, 125.7, 123.3, 123.0, 122.5, 122.1, 118.9, 116.9, 115.8, 113.7, 113.4, 96.4, 95.6, 93.7, 87.3, 86.3, 83.6, 77.9, 77.4, 76.8, 71.1, 70.9, 70.8, 69.7, 69.1, 69.0, 56.3, 34.9 and 31.5. Found: M^+ (MALDI) m/z 866.8. $\text{C}_{57}\text{H}_{70}\text{O}_7$ requires 867.1.

The synthetic procedure used for **G2Cr**, **G3Cr**, **G1Tp**, **G2Tp**, and **G3Tp** was similar to that for **G1Cr**.

G2Cr. 67%, a yellow solid. δ_{H} (250 MHz, CDCl_3) 7.88 (1 H, s), 7.83 (1 H, s), 7.77 (1 H, s), 7.42–7.39 (12 H, m), 7.17 (1 H, d, J 8.6), 7.12–7.10 (4 H, m), 6.84 (1 H, d, J 8.6), 4.20–4.16 (4 H, m), 3.99–3.93 (13 H, m), 3.76–3.69 (12 H, m) and 1.29 (72 H, s). δ_{C} (62.5 MHz, CDCl_3) 159.4, 159.3, 151.0, 149.9, 148.6, 137.43, 137.2, 132.4, 132.2, 128.8, 128.6, 127.8, 127.2, 126.5, 126.1, 126.0, 125.8, 123.4, 123.3, 123.0, 122.5, 122.5, 122.1, 122.1, 118.9, 118.8, 118.5, 117.0, 115.8, 114.0, 113.8, 113.5, 112.9, 96.8, 96.5, 95.9, 94.1, 93.9, 93.4, 90.8, 88.3, 87.3, 87.2, 86.4, 86.3, 83.6, 71.1, 70.9, 70.9, 69.7, 69.2, 69.1, 56.4, 34.9 and 31.5. Found: $(\text{M} + 1)^+$ (MALDI) m/z 1552.1. $\text{C}_{107}\text{H}_{122}\text{O}_9$ requires 1552.0.

G3Cr. 59%, a brown solid. δ_{H} (250 MHz, CDCl_3) 8.02–7.77 (7 H, m), 7.39–7.36 (24 H, m), 7.20–7.08 (9 H, m), 6.85 (1 H, d, J 8.6), 4.20 (4 H, m), 4.01–3.92 (25 H, m), 3.78–3.62 (12 H, m) and 1.27–1.26 (144 H, m). δ_{C} (62.5 MHz, CDCl_3) 159.6, 159.6, 159.4, 159.3, 150.9, 149.6, 148.4, 137.7, 137.4, 137.2, 132.4, 132.2, 128.8, 128.6, 127.8, 127.7, 127.3, 127.2, 126.8, 126.1, 125.9, 125.8, 123.3, 122.9, 122.5, 122.1, 118.9, 118.8, 118.5, 118.4, 118.3, 116.6, 115.9, 114.0, 113.8, 113.4, 113.3, 113.2, 112.9, 112.8, 96.7, 96.4, 95.8, 94.3, 94.1, 94.0, 93.9, 93.8, 93.6, 93.4, 93.3, 91.2, 90.9, 90.7, 88.5, 88.3, 88.2, 87.3, 87.2, 86.4, 86.3, 83.6, 70.8, 69.5, 68.7, 56.4, 34.9 and 31.5. Found: M^+ (MALDI) m/z 2945.3. $\text{C}_{207}\text{H}_{226}\text{O}_{13}$ requires 2921.9.

G1Tp. Whether using **G1OTf** or **G1A** (the alternative route) as the reactant, the synthetic procedure is similar to that of **G1Cr**. The yields were 39 and 71%, respectively. δ_{H} (400 MHz, CDCl_3) 8.73 (2 H, ddd, J 4.8, 1.6 and 1.2), 8.62 (2 H, dt, J 7.6 and 1.2), 8.61 (2 H, s), 7.87 (2 H, td, J 7.6 and 1.6), 7.76 (1 H, s), 7.40 (6 H, m), 7.35 (2 H, ddd, J 7.6, 4.8 and 1.2), 7.12 (1 H, s), 3.98 (3 H, s) and 1.27–1.25 (36 H, m). δ_{C} (100 MHz, CDCl_3) 159.6, 155.9, 155.7, 151.1, 150.9, 149.4, 137.4, 137.1, 133.6, 128.2, 126.2, 126.1, 124.2, 123.5, 123.1, 123.0, 122.5, 122.0, 121.5, 119.0, 113.9, 112.3, 96.9, 93.9, 89.6, 87.2, 86.1, 56.3, 35.0, 31.5 and 31.5. Found: C, 85.03; H, 7.53; N, 5.04%. Found: $(\text{M} + 1)^+$ (LRFAB) m/z 789. $\text{C}_{56}\text{H}_{57}\text{N}_3\text{O}$ requires C, 85.35; H, 7.29; N, 5.33%; M, 787.5.

G2Tp. 78% using **G2OTf** as the reactant and 42% using **G2A** as the reactant. δ_{H} (400 MHz, CDCl_3) 8.74 (2 H, ddd, J 4.8, 1.6 and 1.2), 8.63 (2 H, dt, J 7.6 and 1.2), 8.62 (2 H, s), 7.88 (2 H, td, J 7.6 and 1.6), 7.85 (1 H, s), 7.83 (1 H, s), 7.79 (1 H, s), 7.40–7.34 (14 H, m), 7.13 (1 H, s), 7.10 (1 H, s), 7.09 (1 H, s), 4.01 (3 H, s), 3.93 (3 H, s), 3.92 (3 H, s) and 1.27–1.25 (72 H, m). δ_{C} (100 MHz, CDCl_3) 159.8, 159.5, 159.4, 156.0, 155.8, 151.1, 151.0, 151.0, 149.4, 137.8, 137.5, 137.2, 137.1, 133.6, 127.9, 127.8, 127.3, 126.2, 126.0, 124.2, 123.4, 123.3, 123.2, 123.0, 122.9, 122.6, 122.6, 122.3, 122.2, 121.5, 119.0, 118.9, 118.7, 114.2, 113.9, 113.9, 113.5, 113.1, 113.0, 112.8, 96.9, 96.5, 94.0, 94.0, 93.8, 93.5, 93.2, 91.4, 89.5, 89.4, 88.5, 87.4, 87.3, 86.5, 86.3, 56.5, 56.4, 56.4, 35.0, 34.9 and 31.5. Found: C, 86.07; H, 7.74; N, 2.78%; $(\text{M} + 1)^+$ (MALDI) m/z 1473.5. Calc. for $\text{C}_{106}\text{H}_{109}\text{N}_3\text{O}_3$: C, 86.43; H, 7.46; N, 2.85%; M, 1471.8.

G3Tp. 60%, a brown powder. δ_{H} (400 MHz, CDCl_3) 8.73 (2 H, ddd, J 4.8, 1.6 and 1.2), 8.634 (2 H, dt, J 7.6 and 1.2), 8.629 (2 H, s), 7.89 (1 H, s), 7.88 (2 H, td, J 7.6 and 1.6), 7.87 (1 H, s), 7.85 (2 H, s), 7.82 (1 H, s), 7.810 (1 H, s), 7.808 (1 H, s), 7.40–7.32 (26 H, m), 7.15 (1 H, s), 7.13 (1 H, s), 7.12 (1 H, s), 7.08 (2 H, s), 7.07 (2 H, s), 4.03 (3 H, s), 3.93–3.90 (18 H, m) and 1.27–1.23 (144 H, m). δ_{C} (100 MHz, CDCl_3) 159.8, 159.8, 159.7, 159.5, 159.5, 159.4, 156.0, 155.8, 151.0, 151.0, 150.9, 149.4, 137.8, 137.8, 137.5, 137.5, 137.3, 137.2, 137.1, 133.6, 127.9, 127.8, 127.8, 127.5, 127.3, 127.2, 126.9, 126.2, 126.0, 124.2, 123.3, 123.3, 123.3, 123.2, 122.9, 122.9, 122.6, 122.6, 122.6, 122.6, 122.3, 122.2, 122.2, 121.5, 119.0, 118.9, 118.9, 118.7, 118.6, 118.5, 114.2, 114.1, 113.9, 113.9, 113.6, 113.5, 113.3, 113.0, 112.9, 112.8, 96.8, 96.7, 96.5, 96.4, 94.2, 94.1, 94.0, 93.9, 93.8, 93.5, 93.4, 93.3, 91.4, 91.3, 91.0, 89.5, 88.6, 88.5, 88.4, 87.4, 87.4, 87.3, 87.3, 86.5, 86.5, 86.4, 86.3, 56.6, 56.5, 56.5, 56.4, 35.0, 34.9 and 31.5. Found: C, 86.92; H, 7.63; N, 1.42%; $(\text{M} + 1)^+$ (MALDI) m/z 2841.6. Calc. for $\text{C}_{206}\text{H}_{213}\text{N}_3\text{O}_7$: C, 87.03; H, 7.55; N, 1.48%; M, 2840.6.

2G2A

This compound was isolated as a side product in the reaction of compound **3** (0.0519 g, 0.136 mmol) with **G2A** (0.204 g, 0.165 mmol). Yield 17%. δ_{H} (400 MHz, CDCl_3) 7.84 (2 H, s), 7.81 (2 H, s), 7.74 (2 H, s), 7.39–7.36 (24 H, m), 7.09–7.08 (6 H, m), 3.97 (6 H, s), 3.91 (12 H, m) and 1.27–1.26 (144 H, m). δ_{C} (100 MHz, CDCl_3) 160.8, 159.5, 159.4, 151.0, 151.0, 151.0, 151.0, 138.1, 137.5, 137.2, 128.0, 126.2, 126.0, 123.4, 123.3, 123.0, 122.9, 122.6, 122.5, 122.2, 122.1, 119.0, 118.9, 118.8, 118.7, 114.1, 113.9, 113.8, 113.4, 112.9, 112.2, 96.9, 96.8, 96.5, 94.0, 94.0, 93.9, 93.0, 91.7, 88.5, 87.3, 87.2, 86.4, 86.3, 80.0, 78.9, 56.4, 56.4, 56.4, 35.0, 34.9 and 31.5. M^+ (MALDI) m/z 2479.7. $\text{C}_{182}\text{H}_{198}\text{O}_6$ requires 2479.5.

G1TpRu

A mixture containing **G1Tp** (0.0371 g, 0.0471 mmol), terpyridine ruthenium trichloride (0.0208 g, 4.7198 mmol), 4-ethylmorpholine (4 drops) and methanol (15 cm^3) was refluxed for 21 h. The resulting dark red solution was cooled to room temperature. After filtration, to the filtrate was added 1.0 g of ammonium hexafluorophosphate and the resulting solution was stirred at room temperature for half an hour. Methanol was then removed *in vacuo*. To the residue was then added water (20 cm^3) and methylene chloride (20 cm^3). The organic layer was separated and washed with water (3 \times 20 cm^3) and the solvent was then evaporated. The deep red residue, which was essentially pure product, was further purified by chromatography on basic aluminium oxide, eluting with methylene chloride and then methylene chloride/methanol (30 : 1) to yield the title compound (0.0539 g, 81%) as red solids. δ_{H} (400 MHz, CDCl_3) 8.64 (2 H, s), 8.61 (2 H, d, J 8.0), 8.36 (2 H, d, J 8.0), 8.20 (1 H, t, J 8.0), 7.92 (1 H, s), 7.80 (2 H, t, J 8.0), 7.70 (2 H, t, J 8.0), 7.42–7.40 (6 H, m), 7.33 (2 H, d, J 5.2), 7.25 (2 H, d, J 5.2),

7.1685 (2 H, t, *J* 6.6), 7.168 (1 H, s), 7.09 (2 H, t, *J* 6.6), 3.98 (3 H, s) and 1.27–1.25 (36 H, m). Found: C, 60.58; H, 5.20%; (M – PF₆[–])⁺ (LRFAB), *m/z* 1267; (M – 2PF₆[–])⁺ (LRFAB), 1123. C₇₁H₆₈F₁₂N₆OP₂Ru requires C, 60.38; H, 4.85%; M, 1412.4.

Acknowledgements

Financial support from the Office of Naval Research (ONR) and the Defense Advanced Research Project Agency (DARPA) are gratefully acknowledged.

References

- (a) G. R. Newkome, C. N. Moorefield and F. Vögtle, *Dendritic Molecules: Concepts, Syntheses, Perspectives*, VCH, Weinheim, 1996; (b) Dendrimers in *Top. Curr. Chem.*, F. Vögtle, vol. ed., Springer, Berlin, 1998, vol. 197; (c) J. M. J. Fréchet and C. J. Hawker, in *Synthesis and Properties of Dendrimers and Hyperbranched Polymers*, Comprehensive Polym. Sci., 2nd Suppl., S. L. Aggarwal and S. Russo, eds., Pergamon, Oxford, England, 1996, pp. 140–206; (d) M. Fischer and F. Vögtle, *Angew. Chem., Int. Ed.*, 1999, **38**, 884–905; (e) D. A. Tomalia, A. M. Naylor and W. A. Goddard III, *Angew. Chem., Int. Ed. Engl.*, 1990, **29**, 138–175; (f) F. Zeng and S. C. Zimmerman, *Chem. Rev.*, 1997, **97**, 1681–1712; (g) S. M. Grayson and J. M. J. Fréchet, *Chem. Rev.*, 2001, **101**, 3819–3868.
- (a) M. Fischer and F. Vögtle, *Angew. Chem., Int. Ed.*, 1999, **38**, 884–905; (b) M. E. Piotti, F. Rivera, R. Bond, C. J. Hawker and M. J. M. Fréchet, *J. Am. Chem. Soc.*, 1999, **121**, 9471–9472; (c) M. Liu and J. M. J. Fréchet, *Pharm. Sci. Technol. Today*, 1999, **2**, 393–401; (d) J. F. G. A. Jansen, E. de Brabander van den Berg and E. W. Meijer, *Science*, 1994, **266**, 1226–1129; (e) E. G. Oosterom, J. N. H. Reek, P. C. Kamer and P. W. N. M. van Leeuwen, *Angew. Chem., Int. Ed.*, 2001, **40**, 1828–1849.
- (a) G. Denti, S. Campagna, S. Serroni, M. Ciano and V. Balzani, *J. Am. Chem. Soc.*, 1992, **114**, 2944–2950; (b) G. M. Stewart and M. A. Fox, *J. Am. Chem. Soc.*, 1996, **118**, 4354–4360; (c) V. Balzani, S. Campagna, G. Denti, A. Juris, S. Serroni and M. Venturi, *Acc. Chem. Res.*, 1998, **31**, 26–34; (d) T. Sato, D.-L. Jiang and T. Aida, *J. Am. Chem. Soc.*, 1999, **121**, 10658–10659; (e) A. R. H. J. Schenning, E. Peeters and E. W. Meijer, *J. Am. Chem. Soc.*, 2000, **122**, 4489–4495; (f) D. Gust, T. A. Moore and A. L. Moore, *Acc. Chem. Res.*, 2001, **34**, 40–48.
- (a) C. Devadoss, P. Bharathi and J. S. Moore, *J. Am. Chem. Soc.*, 1996, **118**, 9635–9644; (b) Z. Xu and J. S. Moore, *Acta Polym.*, 1994, **45**, 83–87.
- (a) S. L. Gilat, A. Adronov and J. M. J. Fréchet, *Angew. Chem., Int. Ed.*, 1999, **38**, 1422–1427; (b) A. Adronov and J. M. J. Fréchet, *Chem. Commun.*, 2000, 1701–1710.
- V. J. Pugh, Q.-S. Hu and L. Pu, *Angew. Chem., Int. Ed.*, 2000, **39**, 3638–3641.
- (a) Z. Peng, Y. Pan, B. Yu and J. Zhang, *J. Am. Chem. Soc.*, 2000, **122**, 6619–6623; (b) Y. Pan, M. Lu and Z. Peng, *Polym. Mater. Sci. Eng.*, 2001, **84**, 780–781.
- J. S. Melinger, Y. Pan, V. D. Kleiman, Z. Peng, B. L. Davis, D. McMorrow and M. Lu, *J. Am. Chem. Soc.*, 2002, **124**, 12002–12012.
- V. Percec, W. D. Cho, G. Ungar and D. J. P. Yeardley, *J. Am. Chem. Soc.*, 2001, **123**, 1302–1315.
- (a) Y. Pan, Z. Peng and J. S. Melinger, *Tetrahedron*, 2003, **59**(29), 5495–5506; (b) Y. Pan, M. Lu, Z. Peng and J. S. Melinger, *J. Org. Chem.*, 2003, **68**, 6952–6958.
- (a) K. Sonogashira, Y. Tohda and N. Hagihara, *Tetrahedron Lett.*, 1975, **16**, 4467–4470; (b) H. A. Dieck and R. F. Heck, *J. Organomet. Chem.*, 1975, **93**, 259–263.
- A. Khatyr and R. Ziessel, *J. Org. Chem.*, 2000, **65**, 3126–3134.
- G. R. Newkome, E. He, L. A. Godinez and G. R. Baker, *J. Am. Chem. Soc.*, 2000, **122**, 9993–10006.
- J. N. Demas and G. A. Crosby, *J. Phys. Chem.*, 1971, **75**, 991–1024.
- A. Juris, V. Balzani, F. Barigelletti, S. Campagna, P. Belser and A. Von Zelewsky, *Coord. Chem. Rev.*, 1988, **84**, 85–277.
- (a) G. A. Crosby, R. J. Watts and D. H. Carstens, *Science*, 1970, **170**, 1195; (b) K. Kalyanasundaram, *Photochemistry of Polypyridine and Porphyrin Complexes*, Academic Press, London, UK, 1992; (c) J. P. Sauvage, J. P. Collin, J. C. Chambron, S. Guillerez, C. Coudret, V. Balzani, F. Barigelletti, L. De Cola and L. Flamigni, *Chem. Rev.*, 1994, **94**, 993–1019.